doi:10.3788/gzxb20184702.0230002

# 用于中红外甲烷检测的压强测量与补偿

刘志伟,李梓文,李亚飞,郑文雪,郑传涛,王一丁

(集成光电子学国家重点联合实验室吉林大学实验区,吉林大学 电子科学与工程学院,长春 130012)

**摘 要**:利用一个波长为 3.291 μm 的室温连续、带间级联激光器和一个有效光程长为 54.6 m 的多通池,研究了用于中红外甲烷检测的压强测量及补偿技术。通过对测得的甲烷直接吸收光谱信号进行洛伦兹吸收线型拟合,测量了吸收池内气体压强并补偿了压强变化对甲烷浓度的影响。利用浓度为$2.1\times10^{-6}$的甲烷气体样品,在$1.33\times10^{4}$~$10.64\times10^{4}$ Pa 的范围内进行了压强标定;对压强为 $9.31\times10^{4}$ Pa、浓度为 $2.1\times10^{-6}$甲烷气体样品的压强测量结果进行阿仑方差分析,结果表明,当积分时间为2.2 s时,压强的测量精度约为 219.5 Pa。在 $1.33\times10^{4}$、$3.99\times10^{4}$和 $6.65\times10^{4}$ Pa 三种不同压强条件下,对浓度分别为 $1.0\times10^{-6}$、$1.2\times10^{-6}$、$1.4\times10^{-6}$、$1.6\times10^{-6}$、$2.1\times10^{-6}$甲烷气体样品的浓度和压强做了 15 组测量,验证了所给出的压强测量和补偿技术的可行性。

**关键词**:传感器技术;气体传感器;红外光谱;甲烷检测;气体吸收;吸收光谱;激光光谱;红外激光器

**中图分类号**:TH83 **文献标识码**:A **文章编号**:1004-4213(2018)02-0230002-6

# Pressure Measurement and Compensation for Mid-infrared Methane Detection

LIU Zhi-wei, LI Zi-wen, LI Ya-fei, ZHENG Wen-xue, ZHENG Chuan-tao, WANG Yi-ding

(*State Key Laboratory on Integrated Optoelectronics, College of Electronic Science and Engineering, Jilin University, Changchun* 130012, *China*)

**Abstract**: A pressure measurement and compensation technique was studied by employing a 3.291 μm Continuous Wave (CW) Interband Cascade Laser (ICL) and a dense-patterned Multipass Gas Cell (MPGC) with an effective optical path length of 54.6 m. The pressure inside the MPGC was measured based on direct Lorentzian absorption line fitting on the measured absorption spectral signal of $CH_4$, and then pressure compensation was made on the masured $CH_4$ concentration. Pressure calibration was performed from $1.33\times10^{4}$ Pa to $10.64\times10^{4}$ Pa using a $2.1\times10^{-6}$ $CH_4$ sample. An Allan deviation analysis of the measured pressure of a $2.1\times10^{-6}$ $CH_4$ at $9.31\times10^{4}$ Pa pressure indicates a measurement precision of ~219.5 Pa with a 2.2 s averaging time. Fiveteen groups of pressure/concentration measurements of $1.0\times10^{-6}$, $1.2\times10^{-6}$, $1.4\times10^{-6}$, $1.6\times10^{-6}$ and $2.1\times10^{-6}$ $CH_4$ samples at different pressures of $1.33\times10^{4}$, $3.99\times10^{4}$ and $6.65\times10^{4}$ Pa were performed, and the results proved the feasibility of the proposed pressure measurement and compensation technique.

**Key words**: Sensor technology; Gas sensor; Infrared spectroscopy; Methane detection; Gas Absorption; Absorption spectroscopy; Laser spectroscopy; Infrared laser

**OCIS Codes**: 300.6340; 300.1030; 300.6390; 300.6360; 120.4820

**Foundation item**: The National Key R&D Program of China (Nos. 2016YFD0700101, 2016YFC0303902, 2017YFB0402800), National Natural Science Foundation of China (Nos. 61775079, 61627823, 61307124), Science and Technology Department of Jilin Province of China (Nos. 20140307014SF, 2017C027), and Changchun Municipal Science and Technology Bureau (No. 14KG022)

**First author**: LIU Zhi-wei (1993—), male, M.S. degree candidate, mainly focuses on infrared gas sensing technology. Email: zhiwei16@mails.jlu.edu.cn

**Supervisor (Contact author)**: ZHENG Chuan-tao (1982—), male, associate professor, Ph.D. degree, mainly focuses on infrared gas sensing technology and system. Email: zhengchuantao@jlu.edu.cn

**Received**: Aug.20, 2017; **Accepted**: Oct.17, 2017

## 0 Introduction

Methane ($CH_4$) with an atmospheric concentration level of $\sim 1.8\times10^{-6}$ in the atmosphere, is the second most abundant constituent responsible for climatic forcing after carbon dioxide ($CO_2$)[1-4]. In comparison with mass spectrometry or gas chromatography, optical methods based on infrared laser spectroscopy[5-9] are advantageous for $CH_4$ sensing in terms of size, time resolution and cost. Tunable infrared Laser Absorption Spectroscopy (TLAS)[10-14] enables non-contact measurements and has proven to be an excellent tool for trace gas detection in various applications. Interband Cascade Lasers (ICLs) provide Continuous Wave (CW) radiation between 3.0 μm and 6.0 μm at room temperature, which initiated a new pathway for mid-infrared sensing. Both single-mode and multi-mode ICLs have been adopted in gas infrared absorption spectroscopy in recent years[15-17]. In a traditional $CH_4$ sensor system, a high-cost pressure controller is required for making the pressure inside the gas cell to be constant. Alternatively, people usually compensate pressure variations on $CH_4$ sensing signal through software, but this requires a pressure meter, which will make the sensor system more complex for practical application.

As we know, a spectroscopic transition of the $CH_4$ molecule is associated with a specific amount of energy. When this energy is measured by means of a spectroscopic technique, the spectroscopic line has a particular lineshape. Numerous factors can contribute to the broadening of spectral lines. The principal sources of broadening are: lifetime broadening, Doppler broadening and pressure broadening. For molecules in the gas phase, the principal effects are Doppler and pressure broadening, which apply to rotational spectroscopy, rotational-vibrational spectroscopy and vibronic spectroscopy. In this paper, the pressure broadening effect, which yields a Lorentzian profile, was utilized. When $CH_4$ molecules absorb infrared light generated with specific wavelength, the pressure variations will influence the shape of Lorentzian profile, which can be described by the Full Width at the Half Maximum (FWHM) of the absorption line. This mechanism was utilized for the pressure measurement with high sensitivity in this paper, and a sensor system with a 54.6-m long Multi-Pass Gas Cell (MPGC) was developed for Lorentzian absorption fitting and pressure calibration. $CH_4$ measurements under different pressures were made to validate the normal operation of this technique.

## 1 Sensor structure

The atmospheric pressure measurement sensor system using mid-infrared $CH_4$ absorption spectroscopy is shown in Fig. 1, which consists of an optical and an electrical sub-system. A 3 291 nm CW, Thermo-Electric Cooler (TEC), Distributed Feedback (DFB) ICL was used as the infrared source in the optical sub-system for targeting the 3 038.5 $cm^{-1}$ $CH_4$ absorption line. The line strength is 2.195 $cm^{-2}$/atm, and the air- and self-broadening coefficients are 0.064 5 $cm^{-1}$/atm and 0.081 $cm^{-1}$/atm, respectively. The laser beam was coupled into a mode matching lens (L), reflected by two plane mirrors ($M_1$ and $M_2$), and entered the MPGC with a 54.6 m optical path length. After 4 3 5 reflections, the output beam was focused onto a TEC Mercury-Cadmium-Telluride (MCT) photodetector (VIGO System, model PVI-4TE-4) using a Parabolic Mirror (PM).

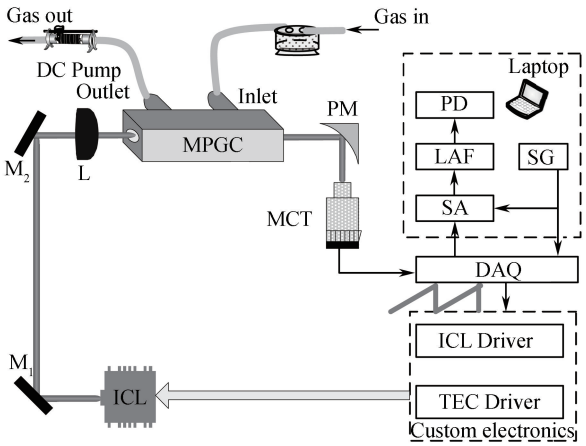


Fig.1 Schematic of a mid-infrared $CH_4$ sensor without a pressure controller based on a CW, TEC ICL

Theelectrical part of the sensor system consists of a laptop (Dell, model # PP04X), a DAQ card (National Instrument, model USB-6356), a custom board-level laser current driver and a temperature controller. The laser driver and temperature controller both have a compact size of $<5\times5$ cm and a supply voltage of +12 V. The temperature controller is capable of operating with an accuracy of $<\pm0.001$ ℃

with a stable temperature drive current. The ratio between input voltage and output current was adjusted to 2.14 mA/V. A laser direct absorption spectroscopy technique was used in $CH_4$ absorption line measurements, which only requires a saw tooth scan signal to drive the ICL. This scan signal was generated by a LabVIEW-controlled DAQ card. The MCT detector signal was sent to the DAQ card for data acquisition, triggered by a signal generation module. A compact DC pump (KNF Neuberger Inc., model UN 85.3 KNDC) was used to pump the target gas into the MPGC.

A LabVIEW based laptop platform was developed and used to process $CH_4$ absorption signals. There are three main functions of this platform: signal generation (SG), Signal Acquisition (SA) and absorption fitting & processing. For the SG sub-system, a scan signal array was generated and supplied to a Digital-to-Analog Converter (DAC) module. The drive signal was applied to the ICL via the DAQ card. For the SA, via the use of an Analog-to-Digital Converter (ADC), the output signal from the MCT detector was sampled at the same sampling rate with the DAC. N frames of spectra were sampled per loop. The sampled N frames were then averaged in order to suppress random noise based on absorption fitting and processing. The background signal was obtained via a fifth-order polynomial fitting using the spectral data without $CH_4$ absorption (i.e. excluding the absorption region). Following normalization on the absorption signal, a Lorentzian Absorption Fitting (LAF) was performed, and the FWHM of the absorption line was derived. The pressure was determined based on the FWHM. The function diagram of the LabVIEW based laptop platform is shown in Fig. 2.

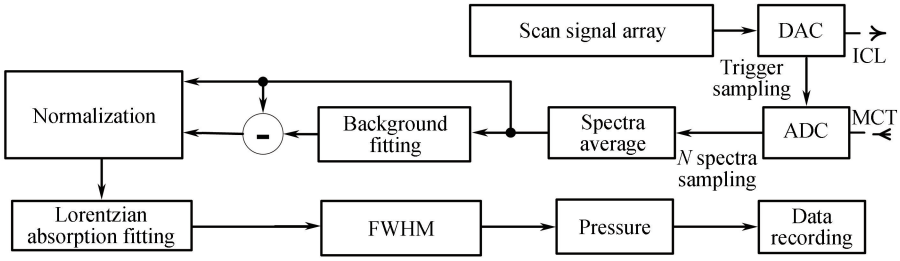


Fig.2 Function diagram of the LabVIEW based laptop platform

## 2 Pressure measurement

In terms of signal processing, $N$ frames of the output signal from the detector $u_r(t)$ were sampled during each calculation loop by means of the DAQ card and averaged as

$$u_{r,\,avr}(t)=\frac{1}{N}\sum_{i=1\sim N}u_{r,i}(t)=\underbrace{u_{r,\,avr}(t)}_{background}-\underbrace{u_{r,\,avr}(t)}_{absorption} \tag{1}$$

Once $u_{r,\,avr}(t)$ was obtained, data fitting based on LabVIEW was used to obtain the background signal

$$u_{r,\,bac}(t)=\underbrace{u_{r,\,avr}(t)}_{background} \tag{2}$$

Furthermore, the following processing was performed to eliminate the background signal

$$u_{r,\,final}(t)=\frac{u_{r,\,bac}(t)-u_{r,\,avr}(t)}{u_{r,\,bac}(t)} \tag{3}$$

Then an absorbance value, considering optical length, gas concentration and absorption coefficient under certain temperature and pressure, is derived by

$$\alpha_{absorbance}(t)=-\ln[1-u_{r,\,final}(t)]=-\ln[u_{r,\,avr}(t)/u_{r,\,bac}(t)] \tag{4}$$

With pressure broadening, $\alpha_{absorbance}(t)$ can be fitted by a Lorentzian signal as

$$\alpha_{r,\,Lorentzian}(t)=\frac{A}{1+4\left(\dfrac{t-t_0}{FWHM}\right)}\xrightarrow{\text{lorentzian absorption fitting}}\alpha_{absorbance}(t) \tag{5}$$

where $A$ represents the absorption intensity, and $t_0$ is the central absorption peak position.

During pressure calibration, the laser temperature was set to 30.95 ℃ using a custom TEC driver. The laser driver current was set to cover from 38 to 45 mA (corresponding to a wavenumber range of 1.624 $cm^{-1}$) to scan the $CH_4$ absorption line at 3 038.5 $cm^{-1}$. This required a ramp scan signal with an amplitude of 3.27 V to be applied to the custom laser driver. Data sampling was triggered by the ramp signal to realize

a complete sample period of the sensing signal, which contains 2 000 points. $N=50$ frames were sampled per calculation loop. All the data were recorded by a laptop for processing and post-analysis.

For the high pressure range of $1.33\times10^4\sim10.64\times10^4$ Pa, the calibration was carried out based on pressure measurements using a standard $2.1\times10^{-6}$ $CH_4$ sample with pure Nitrogen ($N_2$) as balance gas. The FWHM value was recorded for ~10 min for each gas pressure (at $1.33\times10^4$ Pa intervals), as shown in Fig. 3(a). The FWHM value for each pressure was then averaged and plotted as a function of the pressure as depicted in Fig. 3(b). The simulated FWHM values obtained from a HITRAN 2012 simulation were also added in Fig. 3(b) as a comparison with experimental results. Two group values agree well within this range. The relationship between the pressure and the FWHM within a pressure range of $1.33\times10^4\sim10.64\times10^4$ Pa can be represented by a linear curve as

$$P=(6\ 162.97\mathrm{FWHM}-38.54)\times133,\quad P\in[1.33\times10^4,10.64\times10^4\ \mathrm{Pa}) \tag{6}$$

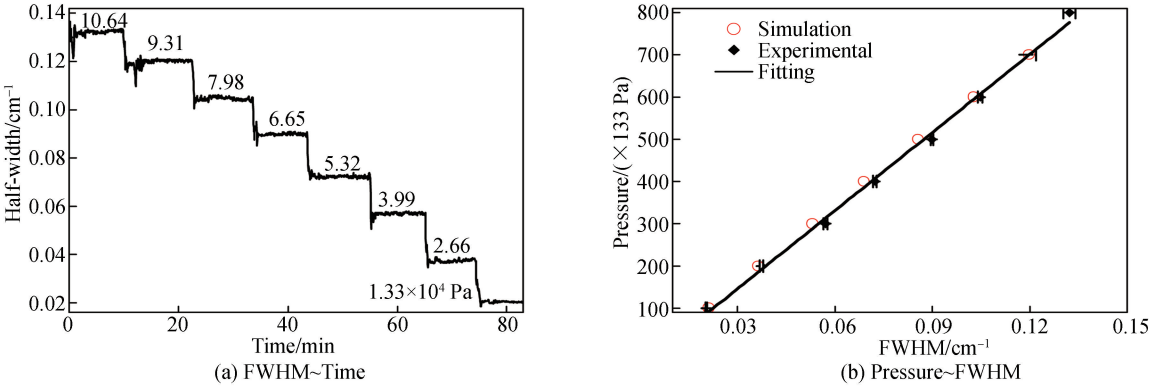


Fig.3 Measured FWHM versus calibration time $t$ and experimental data and fitting curve of gas pressure versus the averaged FWHM

The noise levelof pressure measurements was determined by passing the $2.1\times10^{-6}$ $CH_4$ sample into the gas cell with a controlled pressure of $9.31\times10^4$ Pa and subsequent monitoring of the FWHM. The FWHM was transformed to pressure based on the fitting relation of Eq. (6). A pressure measurement was performed over a time period of ~40 min, as shown in Fig. 4(a). An average pressure of 92 554.7±505.4 Pa (1$\sigma$) was measured for the 40 min observation time. The Allan deviation was plotted on a log-log scale versus averaging time, $\tau$, as shown in Fig. 4(b). The plot indicates a measurement precision of 219.5 Pa with a 2.2 s averaging time. However, the Allan-Werle plot is flat with increasing the averaging time, though it shows a minimum value of 131.7 Pa with an averaging time of 44 s.

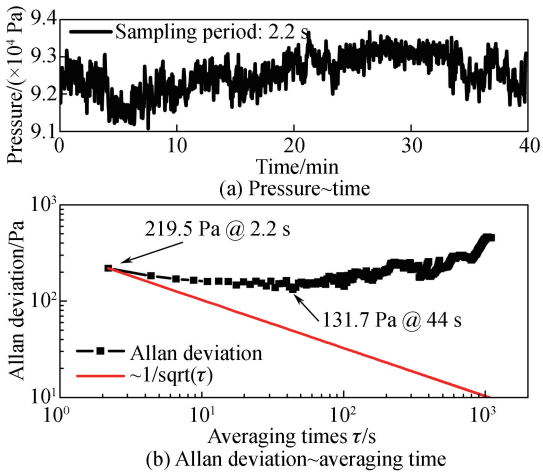


Fig.4 Measured pressure and Allan-Werle deviation plot of a $2.1\times10^{-6}$ $CH_4$ sample with a controlled pressure of $9.31\times10^4$ Pa

## 3 Pressure compensation for $CH_4$ measurement

Experiments were performed to measure the relation between the absorbance and the pressure for a standard $2.1\times10^{-6}$ $CH_4$ sample, which was used as the "calibration gas". The pressure inside the gas cell was controlled at specific levels using the MKS pressure controller. For a pressure range of $1.33\times10^4\sim10.64\times10^4$ Pa, the measured absorbance is shown in Fig. 5. The relation curve can be represented by a fifth-order order polynomial curve within the pressure range of $1.33\times10^4\sim10.64\times10^4$ Pa, as

$$\alpha(P,2.1\times10^{-6})=0.055\ 45+4.196\ 23\times10^{-6}P-1.979\ 14\times10^{-8}P^2+4.538\ 29\times10^{-11}P^3-5.027\ 01\times10^{-14}P^4+2.138\ 53\times10^{-17}P^5 \tag{7}$$

As the increase of pressure, $\alpha$ should continue increasing in theory. The variation of $\alpha$ in the high-pressure range may result from the imperfect Lorentzian absorption fitting due to the change of absorption line shape and broadening mechanism. Based on Fig. 5, at the $CH_4$ absorbance line of 3 038.5 $cm^{-1}$ and a concentration level of $2.1\times10^{-6}$, the absorbance value is 0.088～0.102 within a pressure range of $1.33\times10^4$～$10.64\times10^4$ Pa, indicating a transmission ratio of 0.903～0.915 8, which is calculated by $I/I_0=\exp(-\alpha)$. This absorbance value range is appropriate for the used direct absorption spectroscopy technique, which usually requires an absorbance value of 0.01～0.1.

For an unknown concentration $C$ inside the gas cell, both pressure $P$ and absorbance $\alpha(P, C)$ can be achieved by means of Lorentzian absorption fitting of the absorption peak. Since $\alpha(P,C)\propto C$, we have the following relation at a pressure $P$ as

$$\frac{\alpha(P,C)}{\alpha(P,2.1\times10^{-6})}=\frac{C}{2.1\times10^{-6}} \tag{8}$$

Therefore, we can derive the unknown $CH_4$ concentration with the compensation as

$$C_{com}=\frac{\alpha(P,C)}{\alpha(P,2.1\times10^{-6})}\times(2.1\times10^{-6}) \tag{9}$$

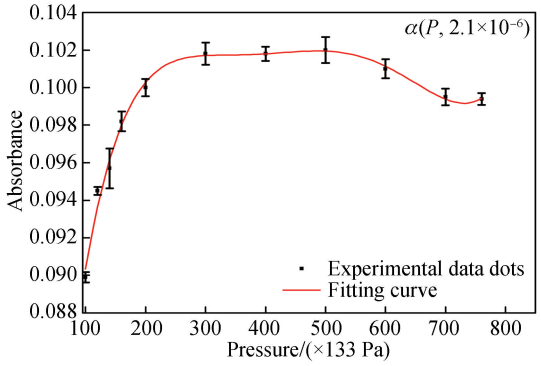


Fig.5 Measured absorbance versus pressure for a $2.1\times10^{-6}$ $CH_4$ sample within the pressure range of $1.33\times10^4$～$10.64\times10^4$ Pa

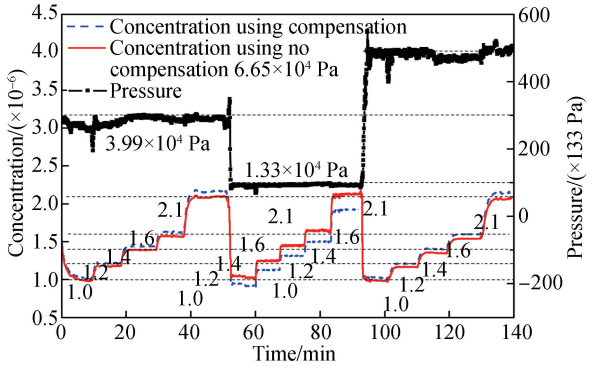


Fig.6 Measured pressure and concentration of five concentration levels of $1.0\times10^{-6}$, $1.2\times10^{-6}$, $1.4\times10^{-6}$, $1.6\times10^{-6}$ and $2.1\times10^{-6}$ at three pressures of $1.33\times10^4$, $3.99\times10^4$ and $6.65\times10^4$ Pa

The sensor performance was further investigated using five diluted $CH_4$ samples with concentration levels of $1.0\times10^{-6}$, $1.2\times10^{-6}$, $1.4\times10^{-6}$, $1.6\times10^{-6}$ and $2.1\times10^{-6}$, by mixing pure $N_2$ and the standard $2.1\times10^{-6}$ $CH_4$ sample. Three groups of measurements were conducted at pressures of $1.33\times10^4$, $3.99\times10^4$ and $6.65\times10^4$ Pa. For each pressure, the $CH_4$ concentration was increased from $1.0\times10^{-6}$ to $2.1\times10^{-6}$. The measured $CH_4$ concentration levels with/without compensation were recorded during the whole monitoring period of 140 min, as shown in Fig. 6. Based on Fig. 5, the absorbance at $1.33\times10^4$ Pa drops more obviously compared to $3.99\times10^4$ and $6.65\times10^4$ Pa, so the effect of pressure compensation is also significant. Moreover, since the whole experiment was carried out continuously by using a pressure controller and a gas dilution system, variations of gas pressure and concentration in the MPGC existed inevitably due to the operation and time-response of the two systems. This leads to the variation of compensated results and some inconsistency between the measurement and the theoretical results. However, in general the compensated $CH_4$ concentration agrees well with the standard value by eliminating the error caused by pressure variations.

## 4 Conclusion

In conclusion, a pressure measurement system using mid-infrared ICL-based $CH_4$ absorption spectroscopy was developed for pressure compensation on $CH_4$ detection without using a high-cost pressure controller or using additional pressure meter. The pressure inside the MPGC was measured using direct Lorentzian absorption line fitting. Pressure calibration experiment was performed from $1.33\times10^4$ to $10.64\times10^4$ Pa using a $2.1\times10^{-6}$ $CH_4$ sample. An Allan deviation analysis of the measured pressure of a $2.1\times10^{-6}$ $CH_4$ at $9.31\times10^4$ Pa pressure indicates a precision of 219.5 Pa with a 2.2 s averaging time.

Pressure/concentration measurements of $1.0\times10^{-6}$, $1.2\times10^{-6}$, $1.4\times10^{-6}$, $1.6\times10^{-6}$ and $2.1\times10^{-6}$ $CH_4$ samples at different pressures of $1.33\times10^{4}$, $3.99\times10^{4}$ and $6.65\times10^{4}$ Pa were performed, and the results indicated the normal function of the proposed pressure measurement and compensation technique.

**References**


[1] KARION A, SWEENEY C, PETRON G, *et al*. Methane emissions estimate from airborne measurements over a western United States natural gas field[J]. *Geophysical Research Letters*, 2013, **40**(16): 4393-4397.

[2] MILLER S M, WOFSY S C, MICHALAK A M, *et al*. Anthropogenic emissions of methane in the United States[J]. *Proceedings of the National Academy of Sciences of the United States of America*, 2013, **110**(50): 20018-20022.

[3] BRANDT A R, HEATH G A, KORT E A, *et al*. Methane leaks from north american natural gas systems[J]. *Science*, 2014, **343**(6172): 733-735 .

[4] SCHWIETZKE S, GRIFFIN W M, MATTHEWS H S, *et al*. Natural gas fugitive emissions rates constrained by global atmospheric methane and ethane[J]. *Environmental Science & Technology*, 2014, **48**(14): 7714-7722.

[5] LANCASTER D G, WEIDNER R, RICHTER D, *et al*. Compact $CH_4$ sensor based on difference frequency mixing of diode lasers in quasi-phasematched LiNbO3[J]. *Optics Communications*, 2000, **175**(4-6): 461-468.

[6] LANCASTER D G, DAWES J M. Methane detection with a narrow-band source at 3.4 μm based on a Nd:YAG pump laser and a combination of stimulated Raman scattering and difference frequency mixing[J]. *Applied Optics*, 1996, **35**(21): 4041-4045.

[7] FISCHER C, SIGRIST M W. Trace-gas sensing in the 3.3 μm region using a diode-based difference-frequency laser photoacoustic system[J]. *Applied Physics B: Lasers and Optics*, 2002, **75**(2-3): 305-310.

[8] RICHTER D, LANCASTER D G, CURL R F, *et al*. Compact mid-infrared trace gas sensor based on difference-frequency generation of two diode lasers in periodically poled LiNbO3[J]. *Applied Physics B: Lasers and Optics*, 1998, **67**(3): 347-350.

[9] PETROY K P, WALTMAN S, DLUGOKANCKY E J, *et al*. Precise measurement of methane in 3.4-μm difference-frequency generation in PPLN[J]. *Applied Physics B: Lasers and Optics*, 1997, **64**(5): 567-572.

[10] SILVER J A. Frequency-modulation spectroscopy for trace species detection: theory and comparison among experimentalmethods[J]. *Applied Optics*, 1992, **31**(6): 707-717.

[11] WERLE P, Review of recent advances in semiconductor laser based gas monitors[J]. *Spectrochimica Acta Part A: Molecular and Biomolecular Spectroscopy*, 1998, **54**(2): 197-236.

[12] SCHILT S, THEVENAZ L, ROBERT P. Wavelength modulation spectroscopy: combined frequency and intensity laser modulation[J]. *Applied Optics*, 2003, **42**(33): 6728-6738.

[13] HE Q, DANG P, LIU Z, *et al*. TDLAS-WMS based near-infrared methane sensor system using hollow-core photonic crystal fiber as gas-chamber[J]. *Optical and Quantum Electronics*, 2017, **49**(3): 115.

[14] YE W, LI C, ZHENG C, *et al*. Mid-infrared dual-gas sensor for simultaneous detection of methane and ethane using a single continuous-wave interband cascade laser[J]. *Optics Express*, 2016, **24**(15): 16973-16985.

[15] JOULLIE A, CHRISTOL P, GaSb-based mid-infrared 2-5 μm laser diodes[J]. *Comptes Rendus Physique*, 2003, **4**(6): 621-637.

[16] MOTYKA M, SEK G, RYCZKO K, *et al*. Optical properties of GaSb-based type II quantum wells as the active region of midinfrared interband cascade lasers for gas sensing applications[J]. *Applied Physics Letters*, 2009, **94**(25): 251901.

[17] VURGAFTMAN I, BEWLEY W W, CANEDY C L, *et al*. Rebalancing of internally generated carriers for mid-infrared interband cascade lasers with very low power consumption[J]. *Nature Communications*, 2011, **2**(1): 585.